Journal of Dynamics, Monitoring and Diagnostics, 2022, 1, 66-83
https://doi.org/10.37965/jdmd.2022.64

ISTP
RESEARCH ARTICLE

Research on Remaining Useful Life Prediction Method of Rolling Bearing Based on Health Indicator Extraction and Trajectory Enhanced Particle Filter

Peng Luo,[1,2] Jiao Hu,[1,2] Lun Zhang,[1,2] Niaoqing Hu,[1,2] and Zhengyang Yin[1,2]
[1]Laboratory of Science and Technology on Integrated Logistics Support, National University of Defense Technology, Changsha 410073, China
[2]College of Intelligence Science and Technology, National University of Defense Technology, Changsha 410073, China

(Received 01 December 2021; Revised 16 March 2022; Accepted 31 March 2022; Published online 02 April 2022)

Abstract: Aiming at the difficulty of mining fault prognosis starting points and constructing prognostic models for remaining useful life (RUL) prediction of rolling bearings, a RUL prediction method is proposed based on health indicator (HI) extraction and trajectory-enhanced particle filter (TE-PF). By extracting a HI that can accurately track the trending of bearing degradation and combining it with the early fault enhancement technology, early abnormal sample nodes can be mined to provide more samples with fault information for the construction and training of subsequent prediction models. Aiming at the problem that traditional degradation rate models based on PF are vulnerable to HI mutations, a TE-PF prediction method is proposed based on comprehensive utilization of historical degradation information to timely modify prediction model parameters. Results from a rolling bearing prognostic study show that prediction starting points can be accurately detected and a reasonable prediction model can be conveniently constructed by the RUL prediction method based on HI amplitude abnormal detection and TE-PF. Furthermore, aiming at the RUL prediction problem under the condition of HI mutation, RUL prediction with probability and statistics characteristics under a confidence interval can be obtained based on the method proposed.

Key words: health indicator; prediction model; prediction starting point; remaining useful life; trajectory-enhanced particle filter

I. INTRODUCTION

As a typical rotating machinery part, rolling bearing is widely used in mechanical equipment. Nowadays, there are many researchers in the fields of rolling bearings' state monitoring [1], fault diagnosis [2], and degradation state identification [3], but relatively few in the field of rolling bearings' remaining useful life (RUL) prediction [4]. Scientific prediction of RUL can effectively improve the safety performance of equipment and maximize the capacity of the equipment. The prognostics of RUL is a systematic project within the Prognostics and Health Management (PHM) [5,6]. It requires a series of preliminary technical work, such as data perception, health indicator (HI) extraction, and state monitoring. Finally, it serves for intelligent operation and maintenance of equipment [7]. The logical relationship is shown in Fig. 1.

As one of the components of PHM, fault prognosis is an indispensable link in the whole chain. Similarly, fault prognosis research requires 'thinking ahead and thinking behind.' The so-called 'thinking ahead' means that fault prognosis needs to be based on fault diagnosis. If the target object is in a healthy state, it does not make sense to predict faults at this point. However, if the target object is on the verge of failure, the significance of fault prognosis will not be obvious. Therefore, it should be further clarified that the fault prognosis work should be based on the early fault diagnosis work. The early fault detection points are obtained by relevant technical strategies, and then the early fault occurrence points of the target object are approached to determine the starting point of fault prognosis. In addition, unlike the condition indicator extracted for fault diagnosis, the appropriate HI needs to be extracted for fault prognosis. HI needs to meet the special requirements of trend stability, consistency of working conditions, and monotonicity, so HI extraction is also an important connotation of fault prognosis. The so-called 'thinking behind' means that the purpose of fault prediction is to provide scientific suggestions for the support decision of follow-up equipment. For the equipment operation and maintenance side, fault prognosis should not only give the RUL of the target object but also carry out uncertainty evaluation of the given prediction results, so as to provide scientific and reasonable prediction results with high confidence for maintenance decision-makers. Around how to realize equipment RUL prediction, researchers have carried out a lot of work and put forward a series of RUL prediction methods. Specifically, the prediction work is based on the extraction of appropriate HI, the determination of the scientific starting point for prediction, and the construction of an appropriate prediction model. The scientific HI can accurately represent the degradation trend of predicted objects and has good monotonicity, robustness, and tendency. To extract the appropriate HI, researchers have carried out a series of research work.

HI types include typical time-domain features and time-frequency features, which are more common than frequency-domain features. Typical time-domain characteristic indexes

Corresponding author: Niaoqing Hu (email: hnq@nudt.edu.cn)

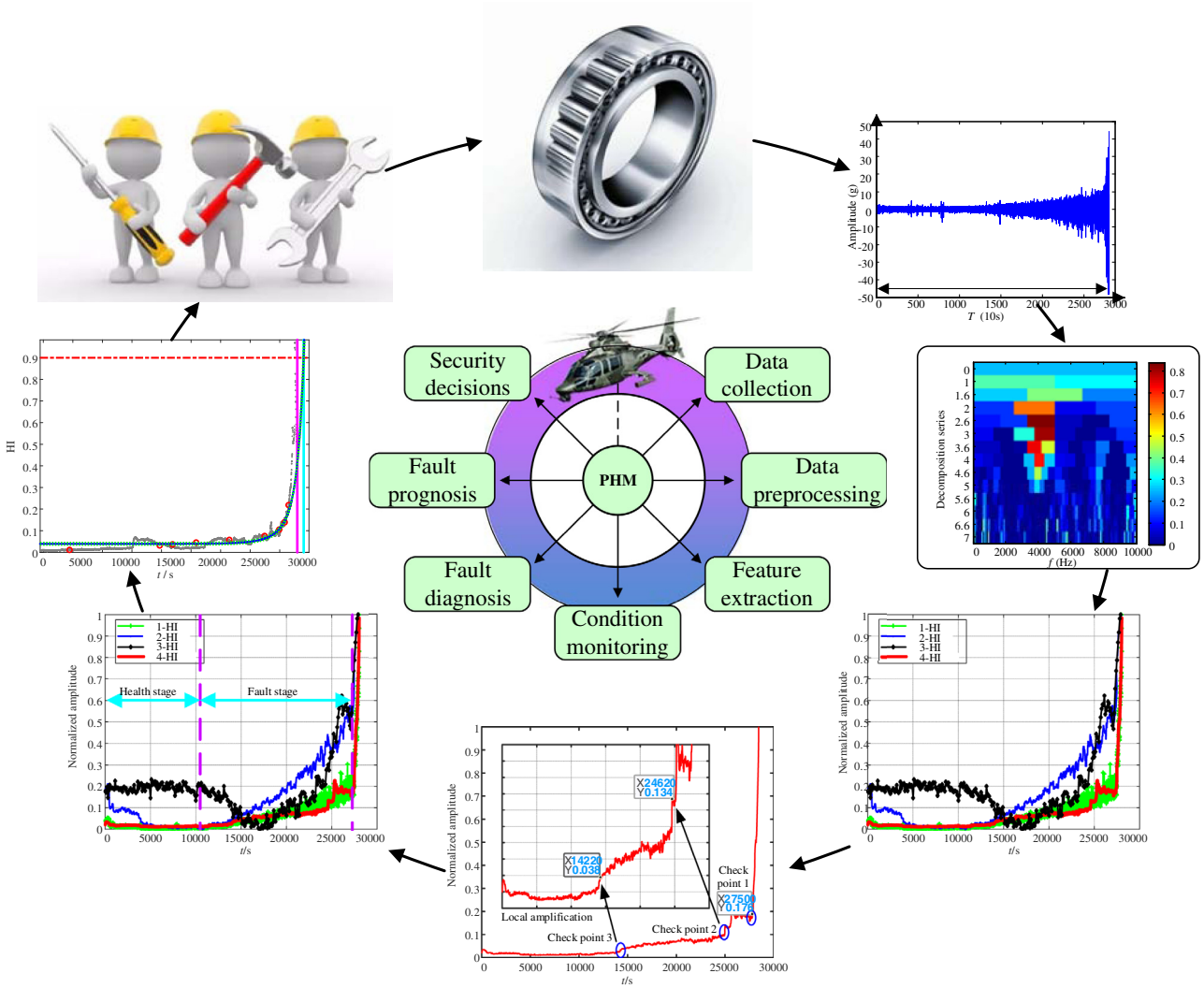

Fig. 1. Logical diagram of equipment RUL prediction.

include waveform indexes, root mean square (RMS), kurtosis indexes, etc. [8], and time-frequency characteristics include various entropy values [9]. In addition to traditional time-domain feature extraction methods, quantitative description methods based on nonlinear signals are also attracting more and more attention from researchers, such as the Lyapunov index [10]. However, the computational efficiency of current algorithms is low and takes a long time [5,11]. With the rise of deep learning methods, HI extraction methods based on deep learning have been mushroomed [12,13]. In which, typical representatives based on deep learning methods, namely the 1-dimensional deep convolutional neural network (1-DDCNN) method, can mine the distributed characteristics of the data adaptively [14]. Then, early fault diagnosis is carried out based on the HI amplitude anomaly detection method.

RUL prediction needs to be established based on the failure of the predicted object. The previous researches on RUL prediction rarely involve the determination of the starting point of prediction. Aiming at this problem, more and more scholars have carried out research on early fault diagnosis. For vibration signals acquired by the early perception of rotating parts' damage, direct fault diagnosis often fails to obtain ideal results, that is, fault features that can accurately characterize early damage cannot be extracted. Therefore, to solve the problem of early weak fault diagnosis of rotating machinery, many researchers and institutions have carried out beneficial exploration.

Due to the periodic impact characteristics of rotating machinery faults, some pulse enhancement methods have been proposed. One typical example is minimum entropy deconvolution (MED) [1]. He et al. [15] proposed a deconvolution method based on modified minimum entropy for early weak fault detection of gears. H. Endo et al. [16] proposed an autoregressive model enhancement method based on MED for early gear fault feature enhancement. Zhang et al. [17] proposed a bearing early fault diagnosis method combining MED and adjustable quality factor wavelet transform to solve the problem of weak impact characteristics of bearing early fault and difficulty in identifying fault information. However, MED methods are easily affected by noise. To solve this problem, maximum correlated kurtosis deconvolution (MCKD) was proposed [18], and more combined methods based on MCKD were derived. Zhu et al. [19] proposed an early bearing fault diagnosis method based on autocorrelation analysis and MCKD. McDonald G L et al. [20] proposed multipoint optimal minimum entropy deconvolution adjusted (MOMEDA), which is used to solve the problem that the bearing fault cycle needs to be preset in advance in the MCKD method. Further, Xia et al. [21]

proposed a fault feature extraction method based on the improved infographic and MOMEDA method. However, the MOMEDA method still needs the prior period of the target object to enhance the periodic pulse.

After the appropriate HI is extracted and the prediction starting point is mined, the RUL prediction can be carried out. Based on the different complexity of research objects, the existing RUL prediction technology can be divided into physical model-based prediction methods, data-driven prediction methods, and hybrid prediction methods [7]. Among them, the prediction method based on a physical model needs profound study on the fault mechanism of the predicted object. For simple predicted objects (such as flat plate and simply supported beam), the prediction method based on a physical model can obtain the ideal prediction accuracy of RUL. However, for complex predicted objects, their failure mechanism is complex, and it is difficult to establish an appropriate failure model. Therefore, physical model-based prediction methods are not competent for the RUL prediction on complex equipment [11]. Thanks to the progress of data perception mean, more degradation state data of complex equipment can be acquired. Then, the data-driven RUL prediction method was born and developed. However, the prediction results of the data-driven prediction method are directly influenced by data, and it is difficult to guarantee the accuracy of prediction when data are missing or not ideal. Furthermore, RUL prediction based on the hybrid method is proposed. Combining the advantages of the physical model-based prediction method and data-driven prediction method, the hybrid prediction method has been widely used in the field of RUL prediction. Among them, the typical representatives of the hybrid methods include the prediction method based on particle filter (PF) [22]. The PF method can optimize the model parameters based on particle updating and obtain the prediction statistical results by extrapolation, and give the prediction results of RUL under the confidence interval, which is more closely related to the actual engineering requirements. Therefore, some researchers have carried out relevant research on how to predict RUL based on the PF method.

Luo et al. [23] and Miao et al. [24] applied the PF method to predict the RUL of lithium batteries. Wang et al. [25] proposed a method for predicting the RUL of equipment based on degradation trajectory. Qian et al. [26] proposed an enhanced particle filtering method for particle degradation. Aiming at the problem that the prediction algorithm takes a long time, Heraldo et al. [27] proposed a method that allows to significantly reduce this computational cost in the case of particle-filter-based prognostic algorithms. Aiming at the problem of the propagation of structural parts crack prediction, Jian et al. [28,29] proposed an online prognostic method for multiple cracks taking advantage of the regularized PF and guided wave-based structural health monitoring and proposed an online updating Gaussian process measurement model within the PF-based crack prognosis framework. Aiming at the problem that the adequacy of the picked process noise has a great influence on the prediction result, Matteo et al. [30] proposed an optimal and unbiased process noise model and a list of requirements that the stochastic model must satisfy to guarantee high prognostic performance. David E. et al. [31] presented a novel prognostic method that allows a proper characterization of the uncertainty associated with the evolution in time of nonlinear dynamical systems based on the PF method, and the proposed algorithm is tested and validated using experimental data related to the problem of lithium-ion battery state-of-charge prognosis. Based on the multisource fusion and monotonicity-constrained particle filtering, He et al. [32] carried out the RUL prediction for the pump. However, the PF method still faces the problems of a large amount of calculation, difficult selections of prediction model, and unstable calculation results [11]. To construct an appropriate prediction model has always been a difficult problem concerned by the researchers of RUL prediction. In the prediction extrapolation stage, there is no observation sample to modify the model, so the prediction model directly determines the prediction results. Simple prediction models are generally difficult to represent the degradation trend of research objects, whereas complex models will inevitably increase the difficulty of prediction methods and calculation costs. Because of this situation, Fan et al. [11] proposed the degradation rate tracking-based particle filter (DRT-PF) method to locate the prediction model parameter as the bearing degradation rate. The parameters to be estimated for particle updating are greatly reduced, and the prediction efficiency is greatly improved, whereas the trend tracking ability of the prediction model is guaranteed. However, in the DRT-PF method, the prediction model parameters at time T are only related to the observed value of the degradation index. As a matter of fact, the parameters of the prediction model at time T are not only determined by the sample observation point at the current time but also by the current degradation trend. If the parameters of the prediction model are only limited to the observed samples at the current moment, it is easy to lose the key information of the historical observed samples and cause the prediction model to deviate from the actual overall degradation trend of the research object.

For the RUL prediction problem of rolling bearing, the overall idea of this paper is shown in Fig. 2. Firstly, an appropriate HI is extracted based on the multi-feature assessment. Secondly, based on the abnormal variation of HI amplitude, the abnormal samples are mined. Furthermore, based on the periodic characteristics of rotating machinery faults, fast spectral kurtosis and MOMEDA methods are used to enhance early fault features, early fault occurrence node is approximated, the starting point of RUL prediction can be determined, and more samples with fault information for subsequent RUL prediction can be provided. Finally, from the perspective of making full use of the trend information of the currently predicted object, the trajectory-enhanced particle filter (TE-PF) method is proposed to predict the RUL. The degradation trend information of the existing samples is comprehensively considered in the process of updating the prediction model parameters, so as to effectively avoid the model distortion caused by the slight mutation of the amplitude of abnormal samples at the current moment.

To sum up, the innovations and contributions of this paper are as follows:

(1) A method for mining the fault prognosis starting points is proposed, which provides more prior knowledge for the establishment of subsequent fault prognosis model;

(2) A TE-PF method, namely TE-PF, is proposed to construct a trend-strengthened fault prognosis model by comprehensively utilizing historical information, which can effectively deal with the fault prognosis problem in the case of HI micro-mutation.

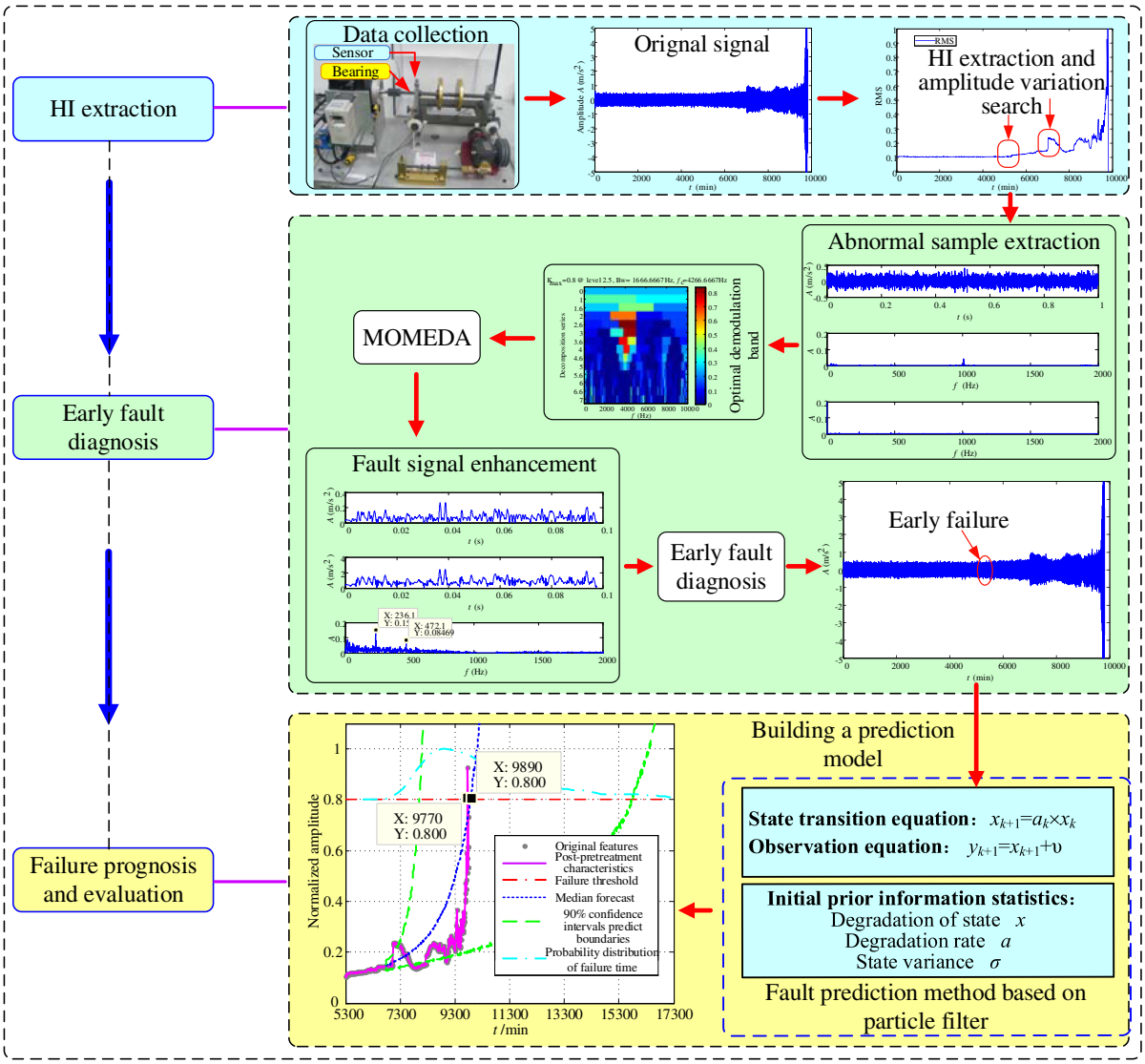

Fig. 2. The overall framework of this paper.

II. EXTRACTION AND EVALUATION OF HI

Based on the idea of the comprehensive evaluation of multiple feature indexes, it is proposed to extract multi-feature indexes for RUL prediction and then evaluate monotonicity, robustness, and tendency, so as to obtain relatively optimal HI by comprehensive evaluation.

Based on the above ideas, the commonly used characteristic indexes as shown in Table 1 are extracted.

Where x_i represents the original time series, T is the measured signal length, and $v(t)$ represents the speed at

Table 1. Commonly used characteristic indexes extracted

Name	Equation	Name	Equation
Mean square value	$\overline{x}^2=\frac{1}{N}\sum_{i=1}^{N}x_i^2$	RMS	$X_{rms}=\sqrt{\frac{1}{N}\sum_{i=1}^{N}x_i^2}$
Waveform indicators	$S=\frac{X_{rms}}{\frac{1}{N}\sum_{i=1}^{N}\lvert x_i\rvert}$	Peak metric	$S=\frac{\max\{\lvert x_i\rvert\}}{X_{rms}}$
Margin index	$L=\frac{\max\{\lvert x_i\rvert\}}{(\frac{1}{N}\sum_{i=1}^{N}\sqrt{\lvert x_i\rvert})^2}$	Pulse index	$I=\frac{\max\{\lvert x_i\rvert\}}{\frac{1}{N}\sum_{i=1}^{N}x_i}$
Kurtosis index	$K=\frac{\frac{1}{N}\sum_{i=1}^{N}x_i^4}{X_{rms}^4}$	Shannon entropy	$H(X)=-\sum_{x}P(x)\log_2[P(x)]$
Vibration intensity	$V_{rms}=\sqrt{\frac{1}{T}\int_0^T v^2(t)dt}$	1DDCNN_HI [14]	$y_{k,m+1}^{j}=f(z_{k,m+1}^{j})$

which the object vibrates. $f(x)=\frac{1}{1+e^{-x}}$, $z_{k,m+1}^{j}=\sum_{n=1}^{Nm} I_{n,m}^{j:j+L_{\ker}} * w_{k,n,m}+b_{n,m}$, $I_{n,m}$ represents the N-th data sample of the M-layer network, there are $n\times m$ of these samples. $I_{n,m}$ can be written as $I_{n,m}^{j:j+L_{\ker}}$, where $L_{\ker}$ represents the convolution kernel size and j represents the j-th point in the sample. $*$ represents convolution algorithm, $w_{k,n,m}$ represents the convolution kernel connecting the N-th sample of m layer and the K-th sample of $M+1$ layer, and $b_{n,m}$ represents the bias. $z_{k,m+1}^{j}$ represents the intermediate output of the convolution layer and $f(\cdot)$ represents the activation function.

To verify whether the extracted HI is scientific and reasonable, the degradation feature evaluation method is introduced into the proposed method to comprehensively evaluate the HI. The main evaluation indexes include monotonicity, robustness, and tendency. The mathematical expression of each evaluation index is as follows:

Monotonicity:

$$Mon_1(X)=\frac{1}{K-1}\left|No.of\ \mathrm{d}/\mathrm{d}x>0-No.of\ \mathrm{d}/\mathrm{d}x<0\right| \tag{1}$$

where $X=\{x_k\}_{k=1:K}$ represents the HI corresponding to the HI sequence x_k in time t_k, K represents the number of the HI, $\mathrm{d}/\mathrm{d}x=x_{k+1}-x_k$ represents the characterize differences in HI sequences, $No.of\ \mathrm{d}/\mathrm{d}x>0$ and $No.of\ \mathrm{d}/\mathrm{d}x<0$ represent the plus and minus of the difference respectively, and $Mon_1(X)$ represents the sum of the derivatives of all HIs X. The monotonicity index evaluation results range from 0 to 1, the higher the score is, the better the monotonicity is.

Robustness:

$$Rob(X)=\frac{1}{K}\sum_{k=1}^{K}\exp\left(-\left|\frac{x_k-x_k^T}{x_k}\right|\right) \tag{2}$$

where x_k^T represents the mean trends of HIs at t_k by smoothing. Similar to the monotonicity evaluation results, the higher the score is, the better the robustness is.

Tendency:

$$Tre_1(X,T)=\frac{K\left(\sum_{k=1}^{K}x_kt_k\right)-\left(\sum_{k=1}^{K}x_k\right)\left(\sum_{k=1}^{K}t_k\right)}{\sqrt{\left[K\sum_{k=1}^{K}x_k^2-\left(\sum_{k=1}^{K}x_k\right)^2\right]\left[K\sum_{k=1}^{K}t_k^2-\left(\sum_{k=1}^{K}t_k\right)^2\right]}} \tag{3}$$

where the range of $Tre_1(X,T)$ is -1 to 1; when it approaches -1 or 1, there is a strong correlation between surface HI and time.

III. RUL PREDICTION STARTING POINT DETERMINATION METHOD

A. BRIEF INTRODUCTION TO THE MOMEDA METHOD

The MOMEDA method constructs an optimal deconvolution filter using the multipoint D-norm as the objective cost function $f=[f_1,f_2,\cdots f_L]$ (where L is the size of the filter) to maximize the target cost function. The specific expression of the target cost function is

$$MDN(y,t,f)=\max_{f}\frac{t^Ty}{\|y\|} \tag{4}$$

where y is the target signal, t is the target vector of the same length as the target signal, and T determines the position and weight of the periodic pulse be convolved. In order to find the maximum MDN, the derivative of the above Eq. (4) about the filter coefficient f is taken, and the process is as follows:

$$\frac{\mathrm{d}}{\mathrm{d}_f}\left(\frac{t^Ty}{\|y\|}\right)=\frac{\mathrm{d}}{\mathrm{d}_f}\left(\frac{t_1y_1}{\|y\|}\right)+\cdots+\frac{\mathrm{d}}{\mathrm{d}_f}\left(\frac{t_{N-L}y_{N-L}}{\|y\|}\right) \tag{5}$$

where N is the length of the original Y; set $\frac{\mathrm{d}}{\mathrm{d}_f}\left(\frac{t^Ty}{\|y\|}\right)=0$, the result can be obtained as follows:

$$\begin{cases}\|y\|^{-1}X_0t-\|y\|^{-3}t^TyX_0y=0\\ \frac{t^T}{\|y\|^2}X_0y=X_0t\end{cases} \tag{6}$$

Based on the $y=X_0^Tf$, and assuming $(X_0X_0^T)^{-1}$ exists, the optimal convolution filter coefficient can be obtained:

$$f=(X_0X_0^T)X_0t \tag{7}$$

$$X_0=\begin{bmatrix}x_L & x_{L+1} & \cdots & x_N\\ x_{L-1} & x_L & \cdots & x_{N-1}\\ \vdots & \vdots & \ddots & \cdots\\ x_1 & x_2 & \cdots & x_{N-L+1}\end{bmatrix}_{L\times(N-L+1)} \tag{8}$$

In order to obtain the pulse period, a series of assumed periods T_m are obtained discreetly within a period range and a series of target vectors t_m are constructed, namely:

$$t_m=\delta_{round(T_m)}+\delta_{round(2T_m)}+\cdots\ \delta_{round(sT_m)} \tag{9}$$

where δ_n represents an impulse at position n in the time series and $round(T_m)$ represents the rounding of the period. Then, a series of deconvolution signals y_m can be obtained, namely:

$$[y_1,y_2\ \cdots\ y_m]=(X_0X_0^T)^{-1}X_0[t_1,t_2\ \cdots\ t_m] \tag{10}$$

Obtain the spectral kurtosis $Mkurt$ of each convolution signal y_m:

$$MKurt=\frac{\left(\sum_{n=1}^{N-L}t_n^2\right)^2\sum_{n=1}^{N-L}(t_ny_n)^4}{\sum_{n=1}^{N-L}t_n^8\left(\sum_{n=1}^{N-L}y_n^2\right)^2} \tag{11}$$

Then, based on the maximum spectrum kurtosis criterion, the fault period is obtained to determine the optimal deconvolution signal.

To sum up, the MOMEDA implementation processes are as follows:

a. Set range vector $\boldsymbol{r}=[r_1\ \cdots\ r_n]$ and window function $\boldsymbol{w}=[1\ \cdots\ 1]$;
b. Compute vectors $\boldsymbol{t}_i(1+m*r_i)=1\ m=0,1,2\ldots$ and store these vectors in matrices $\boldsymbol{T}=[\boldsymbol{t}_1\ \cdots\ \boldsymbol{t}_n]$;
c. Calculate the improved matrix $\boldsymbol{T}^*=\mathrm{filter}(\boldsymbol{w},1,\boldsymbol{T})$;
d. Calculate $\boldsymbol{F}=(\boldsymbol{X}_0\boldsymbol{X}_0{}^{\mathrm{T}})^{-1}\boldsymbol{X}_0\boldsymbol{T}^*$ and $\boldsymbol{Y}=\boldsymbol{X}_0{}^{\mathrm{T}}\boldsymbol{F}$;
e. Select Max Kurtosis $\boldsymbol{y}_i$ from $\boldsymbol{Y}=[\boldsymbol{y}_1\ \cdots\ \boldsymbol{y}_n]$, then this vector $\boldsymbol{y}$ is the best filtering result.

B. THE PREDICTION STARTING POINT MINING METHOD

The prediction starting point is mined based on anomalous HI amplitude detection and MOMEDA. Appropriate HI should be more sensitive to characterize what degradation stage the target object is in, that is to say, the rolling bearing in different fault degradation stages is directly expressed as the amplitude of HI extraction will change accordingly. As shown in Fig. 3, the HIs of rolling bearings are obtained based on degradation data by using four HI construction methods, respectively. Although the evolution trajectory of each HI is different, the key nodes and overall trend change are almost the same. Compared with considering only a single HI, it is more scientific to comprehensively consider multiple HIs' amplitude changes and then fuse the decision.

After obtaining multiple HIs of the target object, early fault diagnosis can be performed based on its amplitude variation. Similarly, taking Fig. 3 as an example, it is obvious that after the rolling bearing goes through the health stage, multiple HI amplitude values begin to fluctuate almost simultaneously, and the rolling bearing enters the fault degradation stage. At this point, relevant fault information can be obtained based on the original samples corresponding to the later degradation stage to guide the discovery of early fault occurrence nodes, which can be called the fault backtracking stage. As shown in Fig. 4, taking 4-HI as an example, original samples of corresponding nodes can be extracted based on the change of HI amplitude in the local enlarged image, and then fault diagnosis can be carried out based on the original samples.

Testing point 1, for example, after extracting 27 050 s corresponding to the original sample data, based on the rapid spectral kurtosis and MOMEDA method, the optimal demodulation frequency band (as shown in Fig. 5) and enhanced envelope spectra (as shown in Fig. 6) can be obtained. By analyzing the characteristic frequency of bearing parts, the rolling bearing fault pattern recognition can be realized. The testing points are gradually moved forward until the fault features cannot be mined. Based on this, the early fault occurrence nodes can be traced, and more observation data with fault information can be provided for the RUL prediction on bearings at the current time, so as to obtain more accurate prediction results of RUL.

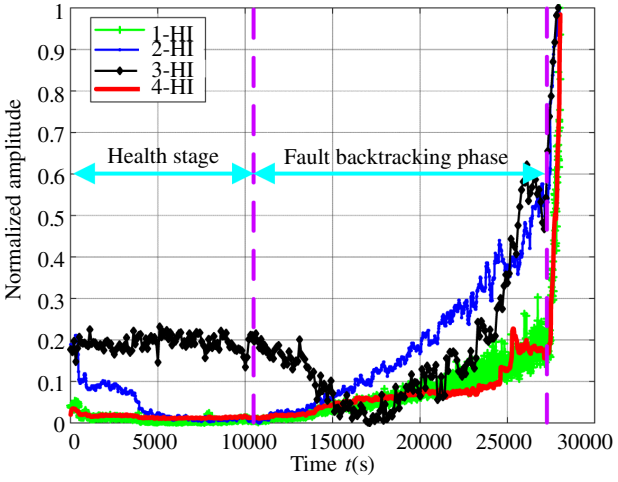

Fig. 3. Normalized HIs obtained by different methods.

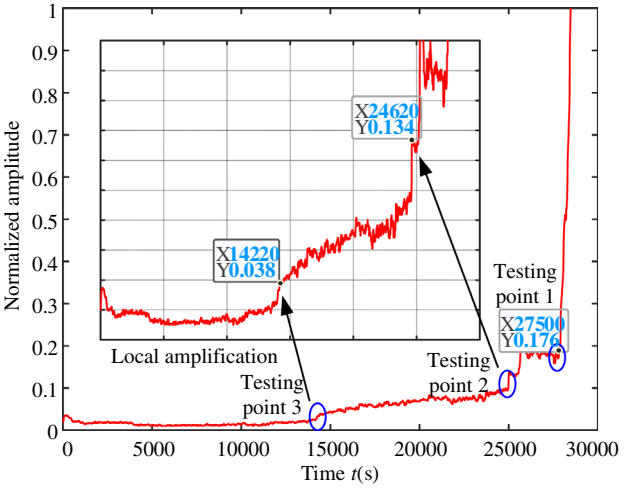

Fig. 4. Local details of 4-HI.

IV. RUL PREDICTION METHOD BASED ON TE-PF

A. INTRODUCTION TO STANDARD PF METHODS

PF is a recursive Bayesian estimation method based on Monte Carlo sampling, which estimates the current state or degradation model parameters of the system recursively through a series of sample observations $y_{1:k} = \{y_1, y_2, \cdots y_k\}$. Generally speaking, the PF method needs to establish a state transition equation and measurement equation of the dynamic system:

$$x_k = f(x_{k-1}, a_k, \omega_k) \tag{12}$$

$$y_k = h(x_k, \eta_k) \tag{13}$$

where x_k and y_k represent the state value and observation value of the system at time k, respectively, and ω_k and η_k

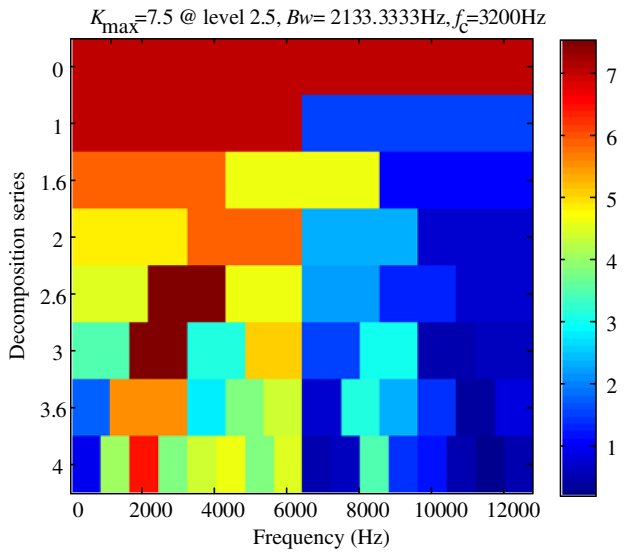

Fig. 5. Optimal demodulation band results obtained based on fast spectral kurtosis method (testing point 1).

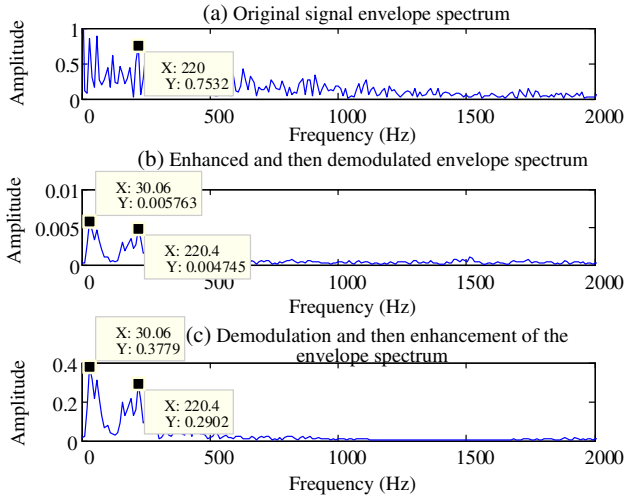

Fig. 6. Envelope spectrum obtained by extraction of original samples based on testing point 1.

represent state noise and measurement noise at time k, respectively.

The PF method mainly includes two steps:

Step 1: Predict the status of the target object. Research object state prediction is carried out based on the prediction model constructed by historical samples and generated samples. The prior probability calculation formula of the existing sample state is as follows:

$$p(x_k|y_{1:k-1}) = \int p(x_k|x_{1:k-1})p(x_{k-1}|y_{1:k-1})dx_{k-1} \tag{14}$$

Step 2: Update the prediction model. Based on the observation value at the current moment, the prior probability is updated to obtain the posterior probability of the system state and then to guide the particle resampling. The posterior probability calculation formula is as follows:

$$p(x_k|y_{1:k}) = p(y_k|x_k)p(x_k|y_{1:k-1})/p(y_k|y_{1:k-1}) \tag{15}$$

where

$$p(y_k|y_{1:k-1}) = \int p(y_k|x_k)p(x_k|y_{1:k-1})dx_k \tag{16}$$

The above formula involves integral calculation, and it is generally difficult to obtain the analytic solution of posterior probability directly. Therefore, the PF method uses a series of particles to approximate the posterior distribution using the Monte Carlo resampler idea, which is called sequential importance sampling (SIS) [17].

The PF method can directly predict the health status of the research object or estimate the parameters of the prediction model, but the former will introduce multidimensional hyperparameters, which greatly increases the uncertainty of the model. The second method, adopted by more researchers, is more straightforward. Therefore, the basic steps of RUL prediction based on the PF method are as follows:

Step 1: Extract the appropriate HI.

Based on the historical life span data of the same research object and the currently observed value, the prediction-oriented feature index extraction research and pretreatment are carried out to construct the trend tracking stable HI.

Step 2: Establish a scientific degradation model.

Based on historical prior knowledge or regression fitting of historical statistical data, an appropriate prediction degradation model is constructed.

Step 3: Establish state transition equation and measurement equation:

$$\begin{cases} a_k = a_{k-1} + \omega_a, \omega_a \sim N(0,\sigma_a) \\ b_k = b_{k-1} + \omega_b, \omega_b \sim N(0,\sigma_b) \\ \cdots \end{cases} \tag{17}$$

$$h_k = f(\theta_k, k) + \eta, \eta \sim N(0,\sigma_0) \tag{18}$$

where $\theta_k = [a_k, b_k, \cdots]$ represents the degradation model parameter vector at time k, and h_k represents the observed value obtained at time k. ω_a, ω_b, and η represent random variables, and σ_a, σ_b, and σ_0 are, respectively, the variance of the above three variables. $f(\cdot)$ represents the degradation model. As the bearing degradation process is complex and changeable, there are many interference factors, not limited to Gaussian noise. Therefore, the PF method is often used in fault prediction of rotating machinery with bearings as an example.

Step 4: Perform degradation model parameter estimation based on the PF method.

Suppose the system has a total of K observation samples, and at each moment of k ($k = 1,2 \ldots K$), prior probability can be updated based on observed samples.

Prediction: At time k, N particles are sampled based on the importance distribution: $\theta_k^i = [a_k^i, b_k^i, \cdots], i = \{1,2, \cdots N\}$ is used to represent the prior distribution of system state;

Update: Calculate the weight of each particle:

$$w_k^i \propto w_{k-1}^i p(y_k|x_k^i) \tag{19}$$

$$\overline{w}_k^i = \frac{w_k^i}{\sum_{i=1}^N w_k^i} \tag{20}$$

The least mean square estimation of system state x at k is

$$\overline{x}_k \approx \sum_{i=1}^N \overline{w}_k^i x_x^i \tag{21}$$

Resampling: Based on the weight size, a new particle set $\{x_{1:k}^{i^*}, i = 1,2, \cdots N\}$ can be obtained.

Step 5: RUL extrapolation prediction based on the prediction model.

By updating the prediction model parameter, the RUL of the research object is extrapolated to obtain the time and the number of particles that reached the set threshold.

Step 6: Evaluation of the uncertainty of prediction results.

The probability statistics of the results obtained in Step 5 are conducted to obtain the probability density distribution function under different failure times, and then the corresponding probability distribution of each RUL prediction time can be obtained, so as to provide decision-makers with prediction results under different confidence levels.

The above expression is the general process of the standard PF method. Compared with other extrapolated prediction methods, the standard PF method is characterized by its ability to provide prediction results under uncertainty evaluation. However, the standard PF method still faces the problem of how to construct a prediction model with strong universality, and the prediction results are largely limited by the updating state of particles, so the stability and the prediction efficiency of the prediction method need to be further improved.

B. BRIEF INTRODUCTION TO TE-PF METHOD

The prediction accuracy and computational efficiency of the standard PF method largely depend on the complexity of the prediction model, that is, the number of parameters to be estimated. The more complex the prediction model is, the more factors it considers comprehensively, and the better its prediction performance will be theoretically. However, the parameters to be estimated in the complex prediction model will increase, and the particle dimension used to estimate the parameters will also increase exponentially, which will inevitably lead to a decrease in computational efficiency and an increase in the instability of the algorithm. On the contrary, the simplified prediction model based on the prediction object has fewer parameters, but its prediction performance will also decrease. The simple model cannot accurately describe the degradation trend of the research object, and the number of parameters of the complex model is bound to be large. In order to reconcile this problem, this paper conducts in-depth research on the modeling and parameter updating of the standard PF method.

In the degradation process of the research object, the degradation trend between two adjacent time series observation samples can be approximated as a linear degradation process. The prediction model based on bearing degradation rate is as follows:

$$x_k = a_{k-1} \times x_{k-1} \tag{22}$$

$$y_k = x_k + \omega_k \tag{23}$$

where y_k is the observed value, x_k is the status value, ω_k is the observation error, and a_{k-1} is the degradation rate of the degraded state, $a_{k-1} = x_k/x_{k-1}$. This prediction model is simple indeed and has a good ability to represent the trend of stable and gradual degeneration processes. However, for the nonstationary degradation process, the prediction model parameters are only determined by the state value at the current moment. Whereas, when the sample state value at the current moment is abrupt, the model will have serious trend distortion. Therefore, the parameter updating method of the above prediction model still needs to be adjusted and improved.

In view of the above problems, the TE-PF method is proposed in this paper, that is, during the process of dynamic adjustment of state model parameters, various useful information is taken into comprehensive consideration, and parameter update of the decision prediction model is integrated.

The prediction model parameter a in the TE-PF method will consist of three parts, namely:

$$a = a_1 + a_2 + a_3 \tag{24}$$

where a_1 is regression predicted value of degradation rate of existing observed samples and particle generation samples, a_2 is the degradation rate of existing observed samples and generated samples and a_3 is the degradation rate of historical observation data.

Instead of simply calculating the ratio between the state value at the later moment and the state value at the previous moment, the state degradation rate values $a_i (i \in [1,2,3])$ at multiple previous moments are calculated and weighted. Weighting values are assigned according to the distance to the current moment. The farther the distance is, the smaller the weight value is. The specific calculation expression of a_i^{k-1} (where k represents the length of the observed samples) is as follows:

$$a_i^{k-1} = w_1 \times \frac{x_2}{x_1} + w_2 \times \frac{x_3}{x_2} + \cdots + w_{k-2} \times \frac{x_{k-1}}{x_{k-2}} (w_1 \le w_2 \le \cdots \le w_{k-2} \,\&\, w_1 + w_2 + \cdots + w_{k-2} = 1) \tag{25}$$

Compared with standard PF methods, the core idea of the TE-PF method is to make full use of the irreversibility and consistency of the trajectory degradation process. For the rotating machinery, taking rolling bearings as an example, when it is in the stage of fault degradation, the degree of failure is irreversible, and the trend of time series information obtained by modern perception means shows a certain stability or degradation law. Ideas based on exponential smoothing suggest that trends in the recent past will continue to some extent into the near future. Therefore, when the parameters of the state transition model are updated, the weights are assigned to the recently acquired parameters. With time forward, the influence of historical data will gradually decrease, and the weight will also become smaller. Based on the above operations, the trend information of existing data can be effectively used to guide and strengthen the trend of particle updating model parameters, and then, a more stable prediction model can be obtained.

To sum up, the overall process of the TE-PF prediction method proposed in this paper is shown in Fig. 7. The basic process is consistent with the standard PF method. Compared with the DRT-PF method, the TE-PF method is still based on the general prediction model constructed by degradation rate. The difference is that the method proposed in this paper estimates the prediction model parameters comprehensively through multiple information and further extrapolates to predict the RUL of the research object in its current state. The probability density distribution of the uncertainty evaluation of the prediction results is given to provide effective decision-making suggestions for equipment maintenance.

V. EXPERIMENTAL VERIFICATION

A. EXPERIMENTAL VERIFICATION BASED ON BEARING DATA SETS WITH DIFFERENT FAULT DEGREES

In order to verify the prediction performance of the TE-PF method, rolling bearing degradation experiments are carried out. The existing public data sets of rolling bearings' full life are generally obtained by accelerating degradation, and there are many uncontrollable factors in the process, such as the running time. Therefore, different from the existing full life accelerated degradation experiment of rolling bearings, this experiment adopts the method of replacing rolling bearings of the same type with different fault degrees to

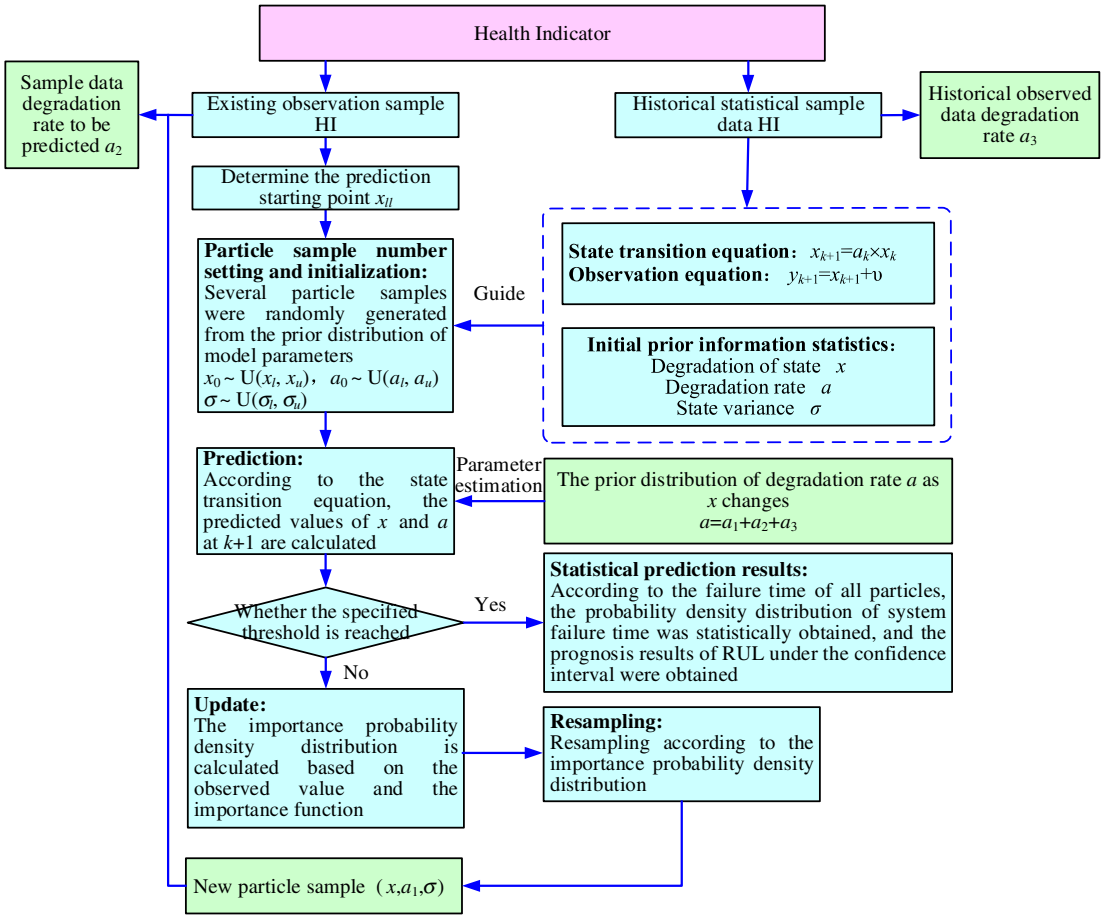

Fig. 7. The overall flow of the TE-PF prediction method.

obtain multisection bearing fault degradation data and then splices to obtain approximate full life degradation data of bearings. The related conditions of the experimental platform and bearing fault parts are shown in Fig. 8. In this experiment, a total of 11 groups of rolling bearings with different degrees of outer ring fault were replaced. Relevant parameters of bearings are shown in Table 2, and related parameters of faulty parts are shown in Table 3. The working speed of each faulty bearing is 600 r/min, the data sampling frequency is 25.6 kHz, the sampling duration of a single sample is 20 s, and the characteristic frequency of bearing outer ring fault is around 30 Hz. The full life degradation data of 220 s long of the testing bearing were obtained by splicing according to the relationship of increasing fault degree. The computing platform parameters are as follows: Processor Model Intel(R) Core(TM) I7–10750H CPU @ 2.60GHz 2.59 GHz.

The above 11 groups of bearing acceleration signals with different outer ring faults are spliced together, and the obtained time-domain waveform of bearing outer ring fault degradation is shown in Fig. 9, and commonly used characteristic indexes as shown in Table 1 are extracted as shown in Fig. 10.

According to the evaluation results of the above characteristic indexes, the comprehensive evaluation indexes of feature No. 7 and feature No. 11 are relatively superior, and the corresponding characteristic indexes are RMS and vibration intensity. The RMS local magnified detail is obtained as shown in Fig. 12. According to the changes in RMS amplitude, the characteristic amplitude at 21 s changed significantly, and the original signal corresponding to this node is taken as the analysis object.

The original time-domain signal at 21 s and its envelope spectrum are obtained as shown in Fig. 13. It is difficult to find the corresponding characteristic frequency of bearing outer ring fault directly and obviously from the envelope spectrum, so it is necessary to conduct fault enhancement processing for the original signal.

Before applying the MOMEDA method to fault feature enhancement, it is necessary to obtain the optimal demodulation frequency band. In this paper, the optimal demodulation frequency band is obtained based on the fast spectrum kurtosis, and the fast spectrum kurtosis of the original signal at 21 s is obtained, as shown in Fig. 14.

According to the spectrum kurtosis shown in Fig. 14, the optimal demodulation center frequency is 666.7 Hz and the frequency bandwidth is 266.7 Hz. Based on the above demodulation frequency information and combined with the MOMEDA method, fault feature enhancement of the demodulation signal is realized and the envelope spectrum of the enhanced signal is obtained, as shown in Fig. 15. In order to compare and verify the fault enhancement effect, the envelope spectrum before and after the enhancement is shown in Fig. 16.

Compared with the envelope spectrum before fault enhancement, 30.01 Hz and its frequency doubling can be obviously found in the envelope spectrum after enhancement. According to the foregoing experimental parameters,

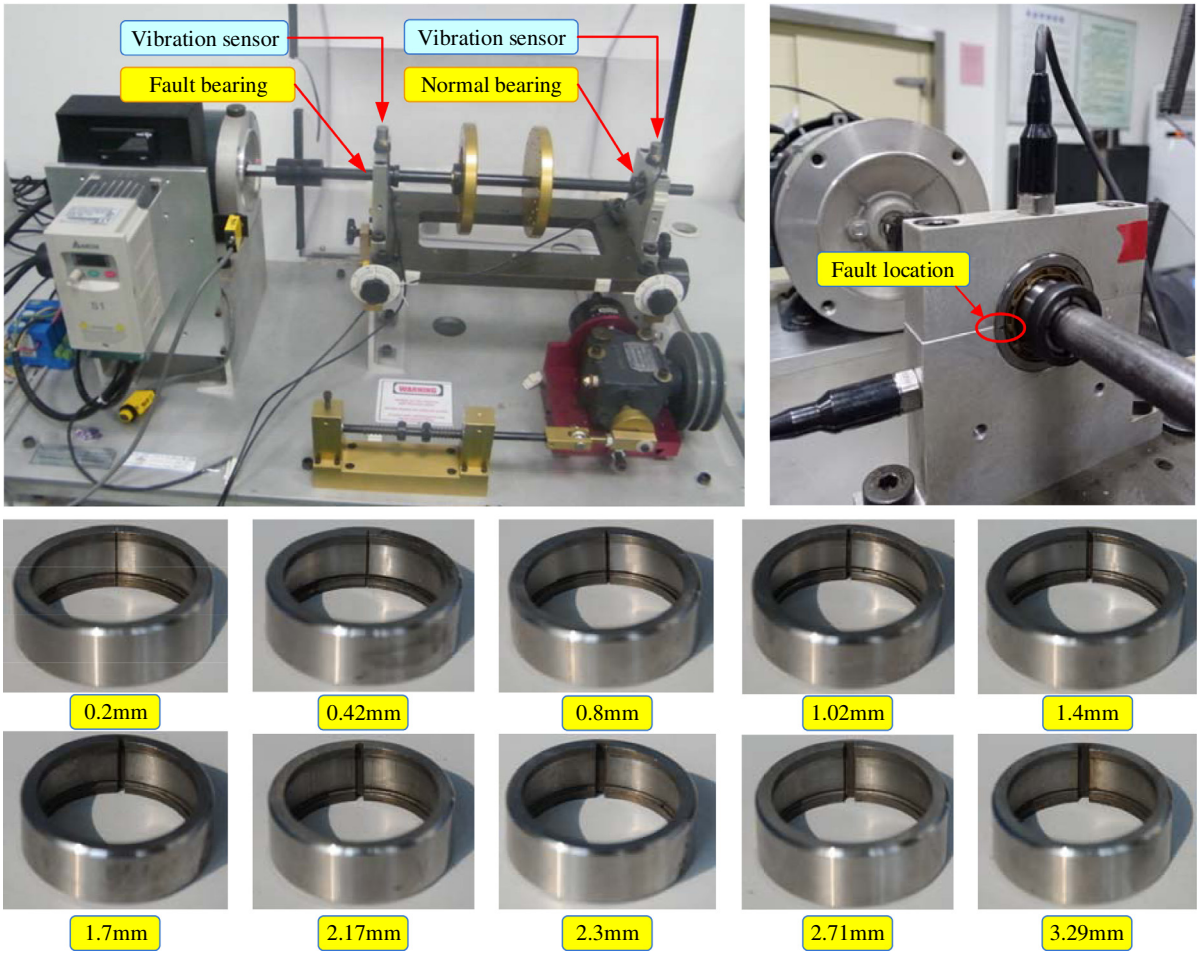

Fig. 8. The experimental platform and fault degree of bearing outer ring.

Table 2. Experimental bearing parameter table

Name	Information
Bearing model	MB ER-10 K
Number of rolling bodies Z	8
Rolling diameter d	0.3125 inches × 25.4 = 7.9375 mm
Pitch diameter D	1.319 inches × 25.4 = 33.5026 mm
Inner raceway diameter $D-d$	25.5651 mm
Outer raceway diameter $D+d$	41.4401 mm
Contact Angle	0

it can be seen that this frequency corresponds to the characteristic frequency 30 Hz of bearing outer ring fault, indicating that the early bearing fault information has been successfully excavated in 21 s, which can provide the starting point for subsequent RUL prediction. Further, the degradation data after 21 s is directly taken as the prediction category, and the corresponding time-domain waveform is shown in Fig. 17.

The data of the first 20 s are healthy signals, and then the fault data are spliced in sequence according to the increasing degree of fault, and finally, the time-domain waveform of class bearing life is obtained. Based on this, follow-up studies are carried out. According to the feature indexes extracted shown in Fig. 10 and the feature evaluation results shown in Fig. 11, it can be seen that the comprehensive evaluation result of vibration intensity is the best. It is obviously inappropriate to directly take the extracted vibration intensity as the HI, and it needs to be processed smoothly. The obtained vibration intensity after pretreatment is shown in Fig. 18.

As shown in Fig. 18, after smoothing, the HI still showed a stage of micro-mutation (taking 45 s and 120 s at the marker as an example). When the prediction start time is at this stage, the standard PF method and DRT-PF method will have trend misdirection, leading to the distortion of the prediction model. In order to verify the superiority of the TE-PF method proposed in this paper, the RUL prediction at the stage of micro-mutation will be carried out.

Table 3. Dimension table of fault parts

Fault location	Slot cutting width /mm	Cutting depth/mm
Outer ring	0.2, 0.42, 0.8, 1.02, 1.4, 1.7, 2.17, 2.3, 2.71, 3.29	0.3

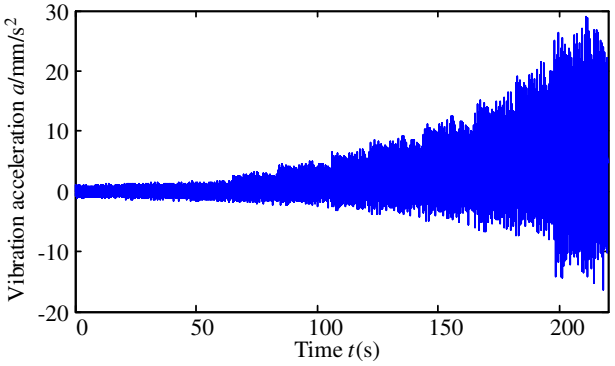

Fig. 9. Full-life time-domain waveform of bearing.

The standard PF method intends to adopt the double-index model with a stronger trend tracking ability as follows [33]:

$$x = a \times \exp(b \times t) + c \times \exp(d \times t) + \delta \tag{26}$$

Based on the historical prior data, the initial distribution interval of each parameter of Eq. (26) are as follows:

$$a \in [1 \times e^{-10}, 1 \times e^{-3}], b \in [0.005, 0.03]$$

$$c \in [0.2, 0.3], d \in [1 \times e^{-4}, 3 \times e^{-3}], \delta \in [0.01, 0.1]$$

And the initial distribution interval of each parameter of Eq. (25) are as follows:

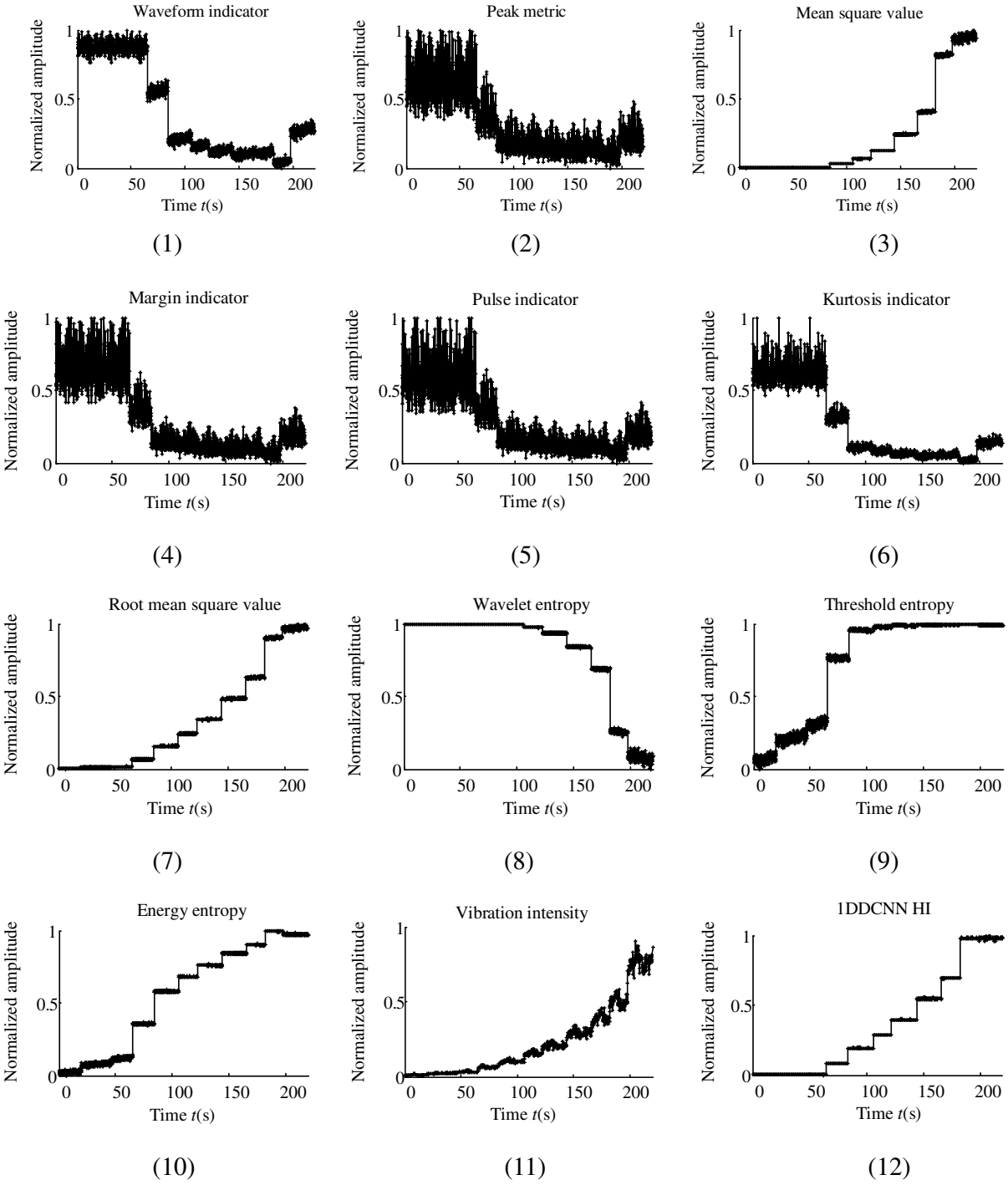

Fig. 10. 12 Characteristic indexes extracted based on bearing full life.

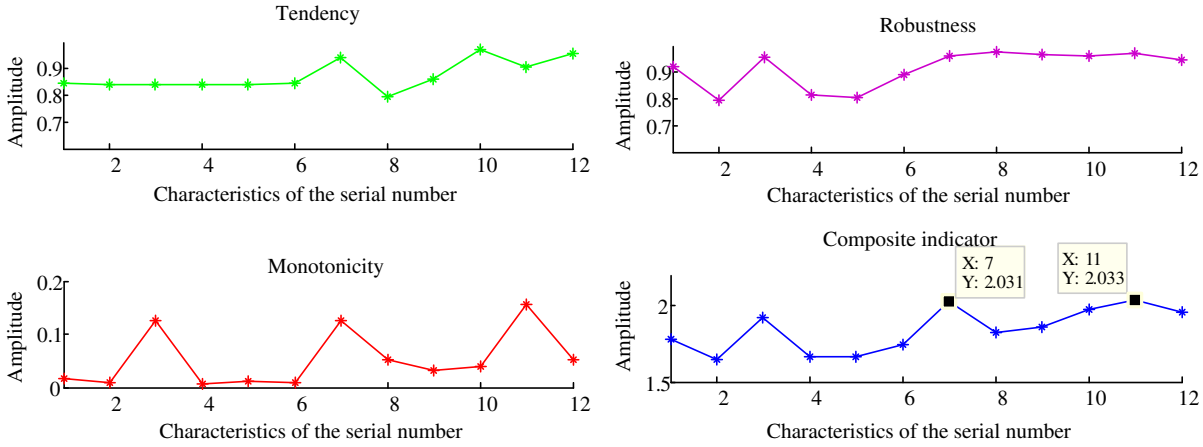

Fig. 11. Evaluation results of characteristic indexes.

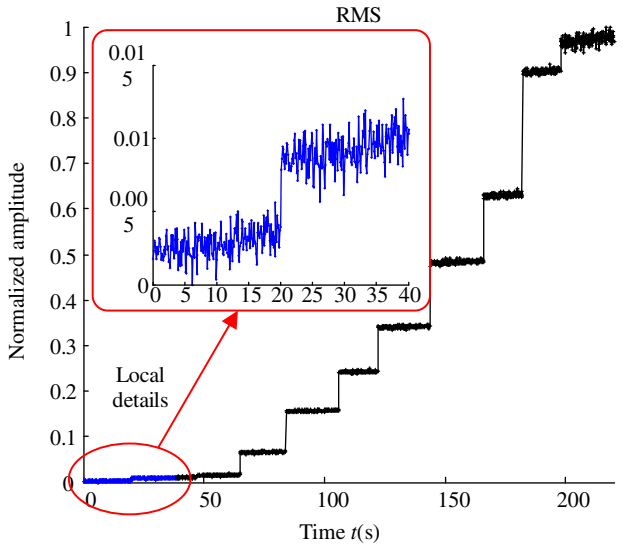

Fig. 12. Local amplification of RMS.

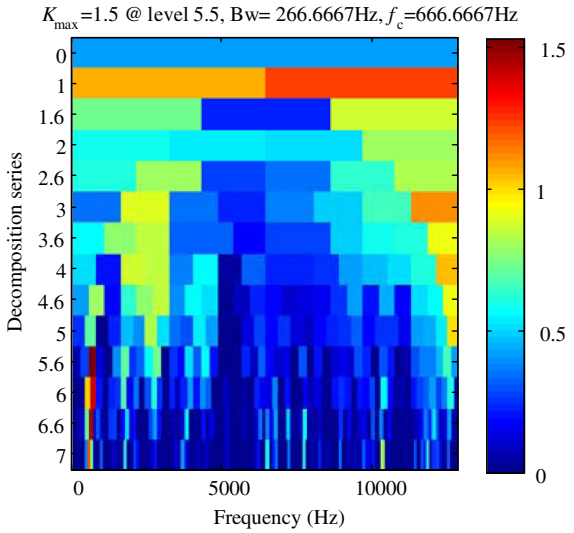

Fig. 14. Rapid spectrum kurtosis corresponding to the 21-s original sample.

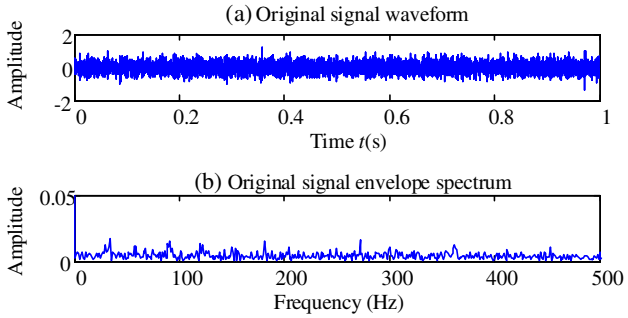

Fig. 13. Original signal and envelope spectrum at 21 s.

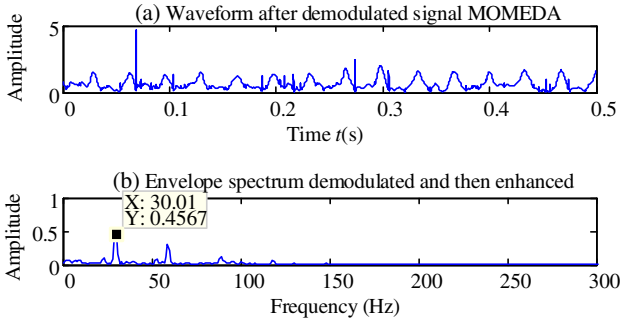

Fig. 15. Demodulation signal and envelope spectrum of fault enhancement.

$$a \in [1,1.03], \delta \in [0.005,0.1]$$

In order to show the probability distribution of RUL estimation results more intuitively, the probability distribution curve in the subsequent prediction graph is appropriately scaled up and shifted. Suppose that the probability density distribution function is $f(x)$, the calculation expression can be as expressed follows:

$$\int f(x)\mathrm{d}x = 1 \tag{27}$$

After translation amplification, the probability density distribution function $f_{new}(x)$ is expressed as:

$$f_{new}(x) = f(x) \cdot [0.2/f(x)] + thres \tag{28}$$

where *thres* is the set failure threshold, and its size is set to 1.

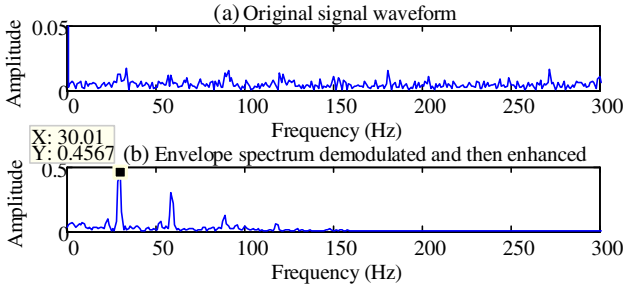

Fig. 16. The contrast of envelope spectrum before and after fault enhancement.

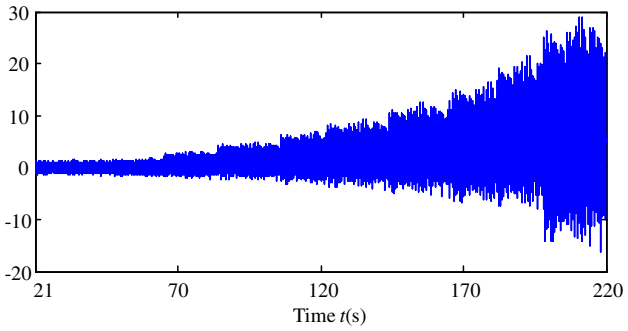

Fig. 17. Vibration intensity waveform extracted from full life degradation data.

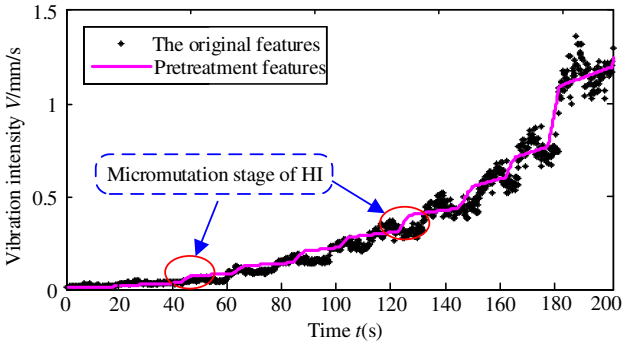

Fig. 18. Original vibration intensity and vibration intensity after pretreatment.

The prediction starting point is selected at 45 s and 120 s, respectively, and the prediction results of the three PF prediction methods are obtained as shown in Figs. 19–24. In which, Figs. 19–21 showed the corresponding prediction results when the prediction starting point is 45 s. Compared with the overall degenerate data, the observed sample at this time is not long enough, so the extrapolated prediction results obtained are not particularly ideal. When the observation sample length increases to 120 s, the prediction effect of the three prediction methods is significantly improved as shown in Figs. 22–24.

Furthermore, to compare and analyze the performance of the three PF methods, the median prediction accuracy and calculation time obtained by the three methods under a 90% confidence interval of different observation sample lengths are summarized in Table 4, where the prediction accuracy calculation expression is shown as follows:

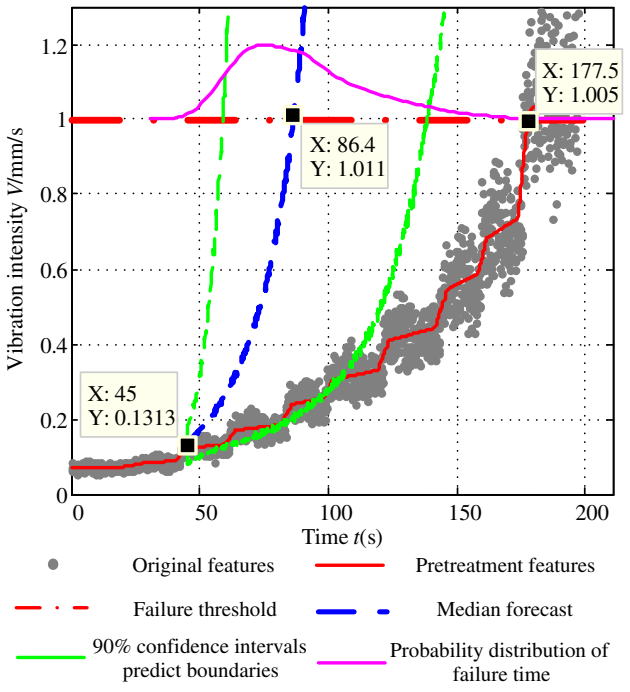

Fig. 19. Prediction results of original PF method under 45 s observation sample duration.

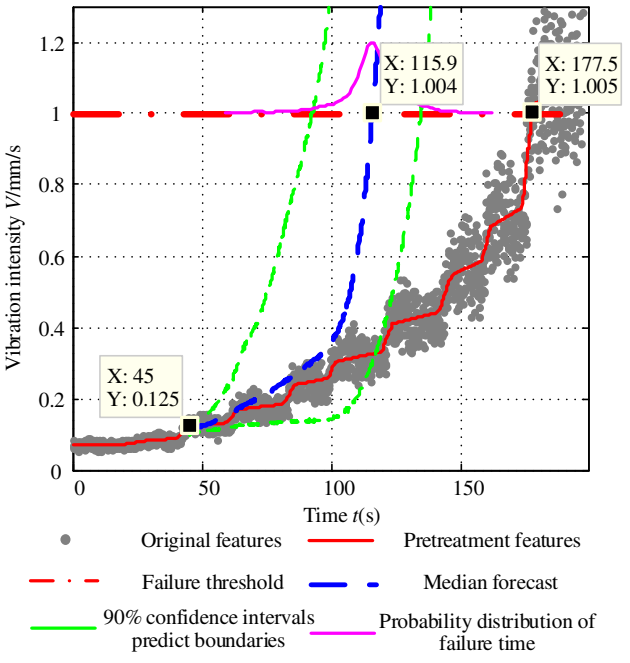

Fig. 20. Prediction results of DRT-PF method under 45 s observation sample duration.

$$Acc = |T_{prediction} - T_{actual}|/T_{actual} \tag{29}$$

where $T_{prediction}$ and T_{actual} represent the predicted failure time and the actual failure time, respectively.

According to the above prediction results, with the increase of the observed sample length, the prediction accuracy of the three prediction methods is improved, and the calculation time is also increased. Compared

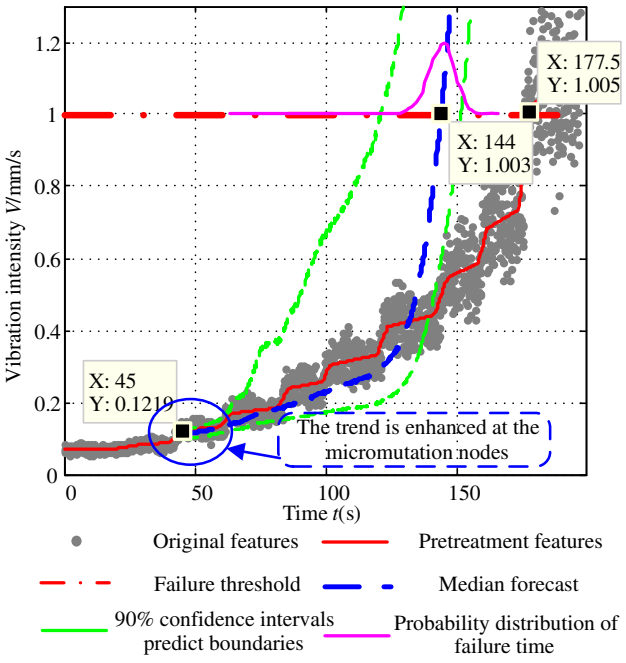

Fig. 21. Prediction results of TE-PF method under 45 s observation time.

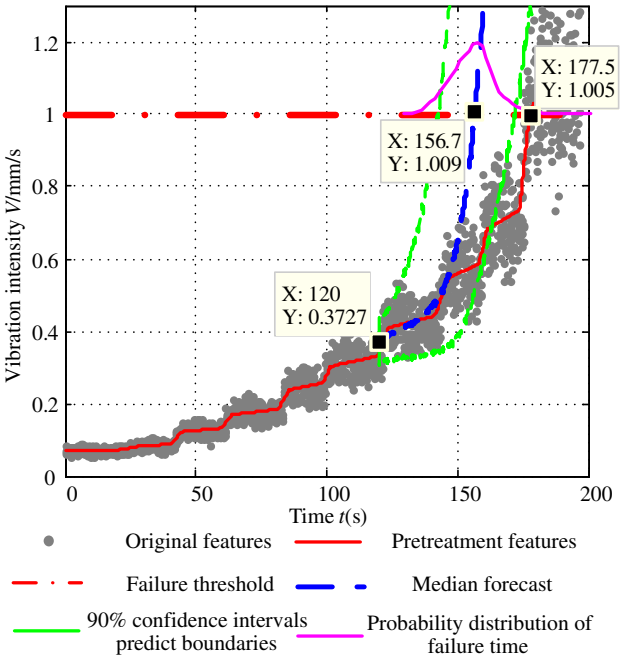

Fig. 23. Prediction results of DRT-PF method under 120 s observation time.

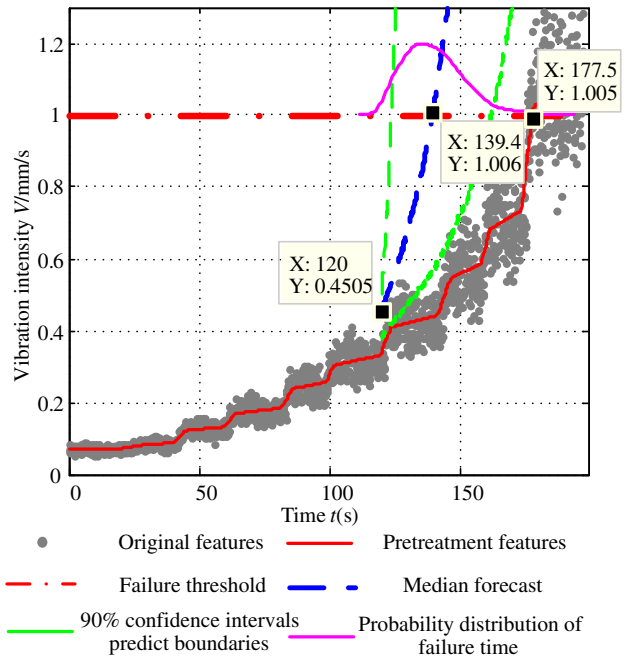

Fig. 22. Prediction results of original PF method under 120 s observation time.

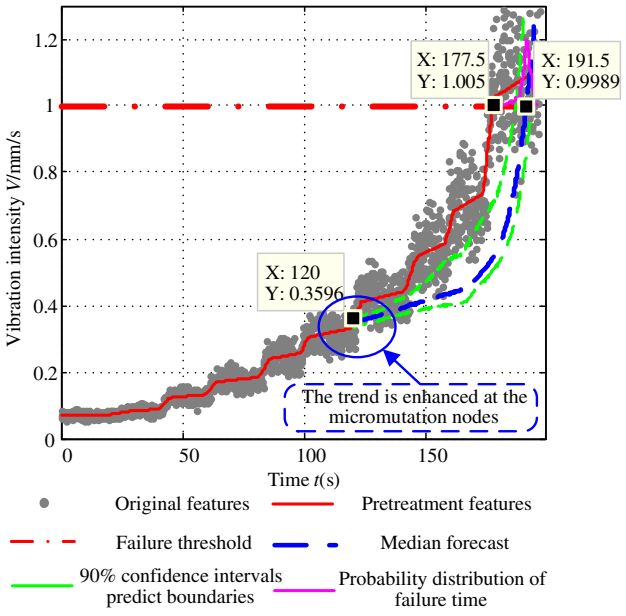

Fig. 24. Prediction results of TE-PF method under 120 s observation time.

with the standard PF method, the DRT-PF method and the TE-PF method have better prediction accuracy when facing the RUL prediction problem at the stage of micro-mutation. When the observation sample length is increased to 120 s, the prediction accuracy of the median value based on TE-PF has reached 92.11% under the 90% confidence interval. In general, compared with the PF method and the DRT-PF method, the TE-PF method proposed in this paper has the most ideal performance.

B. EXPERIMENTAL VERIFICATION BASED ON ACCELERATED DEGENERATE BEARING FULL-LIFE DATA SET

To further verify the prediction performance of the TE-PF method on the accelerated degenerate bearing full-life data set, this paper continues to compare and verify the performance of the above three prediction methods based on the IEEE PHM2012 challenge bearing full-life data set. To obtain the full-life degradation data of bearings in a short time, a radial load of 4000 N was added to the bearings

Table 4. Comparison results of prediction performance of different methods under different observation sample duration

Methods	Duration of observed sample 45 s		Duration of observed sample 120 s	
	Prognosis accuracy (%)	Computing time (s)	Prognosis accuracy (%)	Computing time (s)
Standard PF	48.68	12.78	78.54	13.42
DRT-PF	65.30	14.31	88.28	19.16
TE-PF	81.13	15.41	92.11	18.31

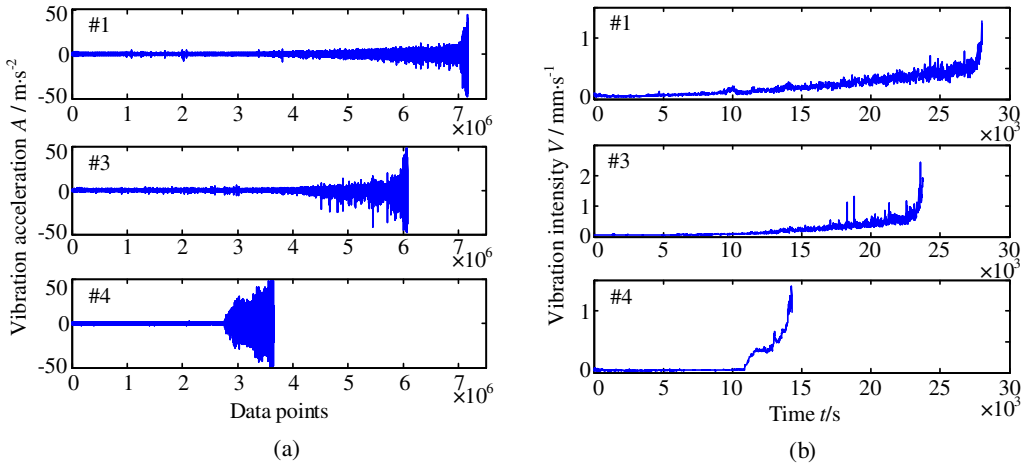

Fig. 25. Original time-domain waveform and vibration intensity extracted.

through cylinder loading in the data set acquisition experiment of the IEEE PHM2012 challenge. Experimental bearing degrades rapidly from a healthy state to failure under extreme conditions. Relevant experimental conditions and data acquisition parameters are as follows: the speed is 1800 r/min, the sampling frequency is 25.6 kHz, the sampling interval is 10 s, and the sampling time of a single sample is 0.1 s. Bearing1-1 data set, Bearing1–3 data set, and Bearing1–4 data set in the data set have a relatively stable gradual trend, so they are selected as method verification objects. Figure 25 shows the time-domain waveform of the above three data sets and the extracted vibration intensity indicator. Taking bearing data set Bearing1-1 and data set Bearing1–4 as training sets, relevant prior knowledge can be obtained. Then, a prediction test is carried out for the Bearing1–3 data set, and the performance of the three prediction methods is compared and analyzed.

It is unscientific to directly use the extracted vibration intensity for prediction, so it needs to be preprocessed. Taking the Bearing1–1 data set as an example, the vibration intensity after pretreatment is shown in Fig. 26. After smoothing, the HI still showed a stage of micro-mutation (e.g. the 2700 s and 10 400 s at the marker). In order to verify the superiority of the TE-PF method proposed in this paper, RUL prediction at the stage of micro-mutation has been carried out.

When the observation sample length is 2700 s, the prediction results of RUL obtained based on standard PF method, DRT-PF method, and TE-PF method are shown in Figs. 27–29, respectively. According to the prediction results, due to the insufficient sample observation length, the prediction accuracy obtained is not very high.

However, compared with the standard PF methods, the DRT-PF method and the TE-PF method have relatively strong trend tracking ability in the initial extrapolation stage.

When the sample observation length is 10 400 s, the prediction results of RUL obtained based on standard PF method, DRT-PF method, and TE-PF method are shown in Figs. 30–32, respectively.

When the observation sample time increases to 10 400 s, obviously, the prediction accuracy of various PF methods can be effectively improved. This is also

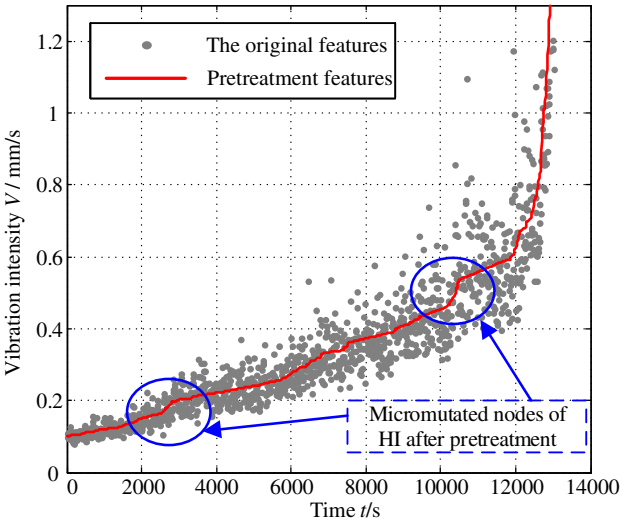

Fig. 26. Original features and features after pretreatment.

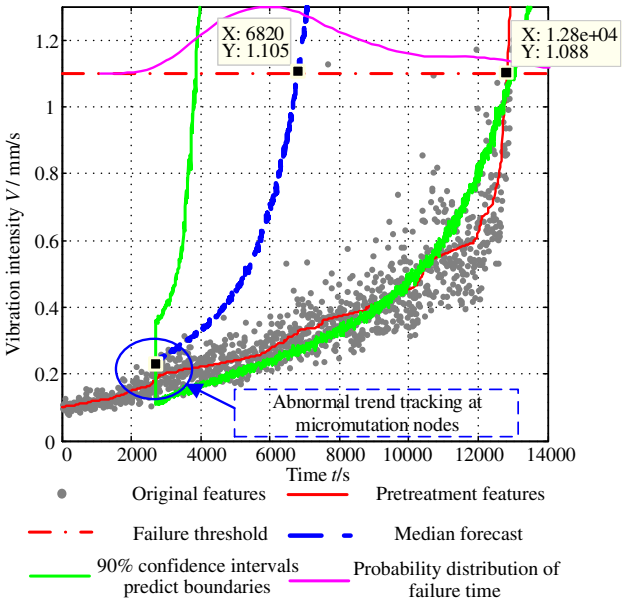

Fig. 27. Prediction results of the standard PF method under 2700 s observation time.

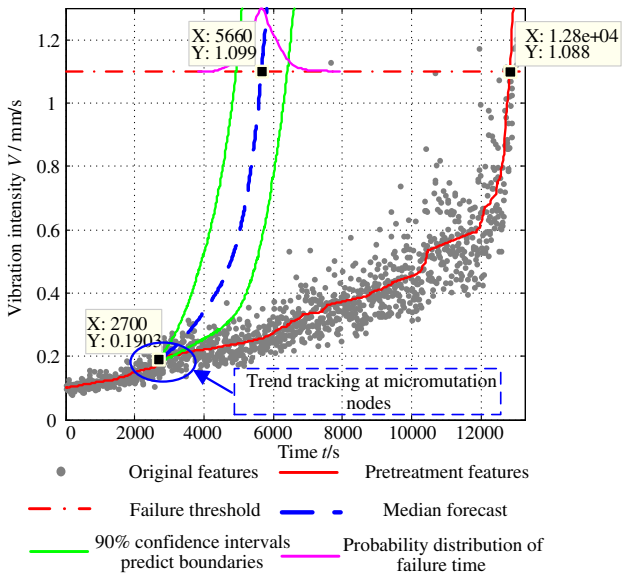

Fig. 28. Prediction results of DRT-PF method under 2700 s observation time.

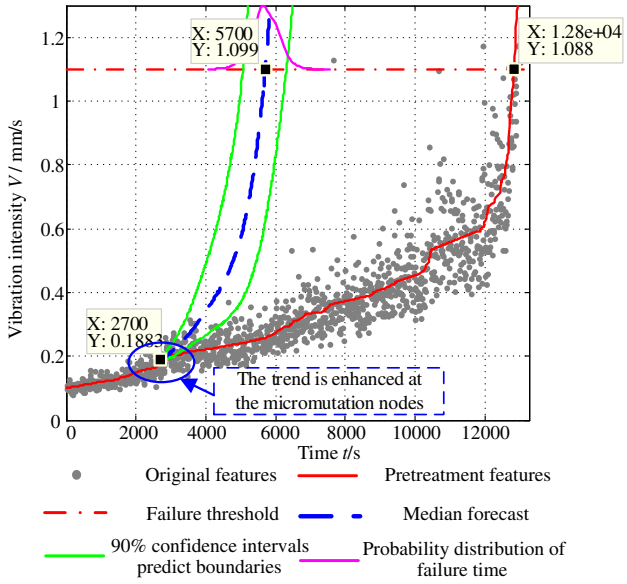

Fig. 29. Prediction results of TE-PF method under 2700 s observation time.

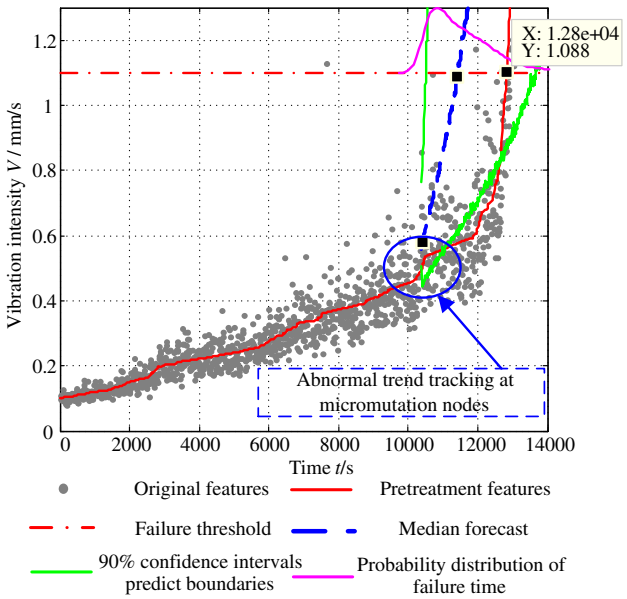

Fig. 30. Prediction results of the standard PF method at 10 400 s.

consistent with the actual law, that is, the more the degradation information obtained, the prediction results will be closer to the actual real results. Compared with the DRT-PF method and TE-PF method, the standard PF method still has a large deviation in the adjustment of the prediction model at the initial stage of extrapolation. While the DRT-PF method is obviously inferior to the TE-PF method in trend tracking performance in the face of a larger HI amplitude mutation. To further compare and analyze the performance of the three PF methods, the median prediction accuracy and calculation time obtained by the three methods under a 90% confidence interval under different observation sample lengths are summarized as shown in Table 5.

As can be seen from the summary results in Table 5, when the number of observed samples is insufficient, the prediction accuracy of all particle filtering methods is not particularly ideal. When the sample observation length increases, the prediction accuracy of each method can be improved effectively. Due to the low parameter dimension of the prediction model, compared with the standard PF method, the computational efficiency of the DRT-PF method and TE-PF method is higher relatively. In face of fault prognosis in the case of small abrupt HI amplitude, the TE-PF method proposed in this paper has both accuracy and computational efficiency advantages and has better comprehensive trend prediction performance.

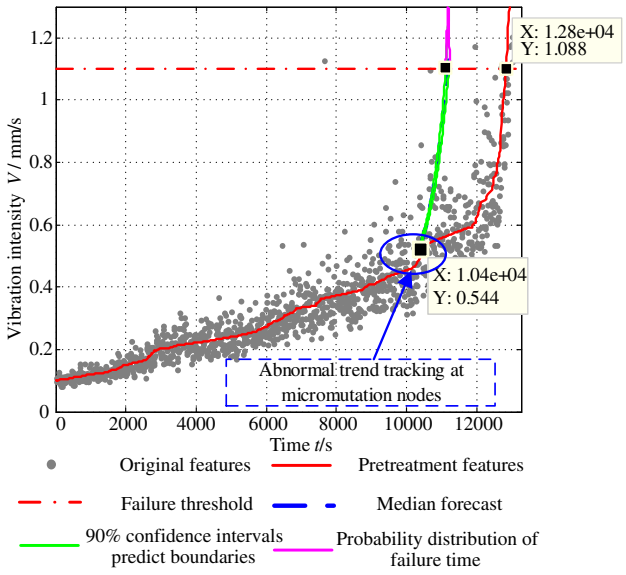

Fig. 31. Prediction results of DRT-PF method under 10 400 s observation time.

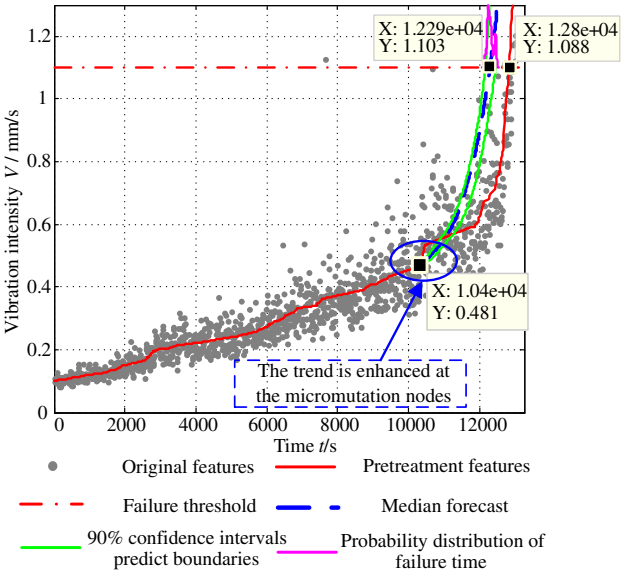

Fig. 32. Prediction results of TE-PF method under 10 400 s observation time.

VI. CONCLUSION

Aiming at the problem of determining the starting point of RUL prediction and the construction of the prediction model, a bearing RUL prediction method based on HI and TE-PF is proposed in this paper. Firstly, by extracting multiple characteristic indexes and carrying out the multi-index evaluation, the HI that can accurately characterize the bearing degradation state is screened and obtained. Secondly, based on the anomalous HI amplitude detection and the MOMEDA fault feature enhancement technology, the original sample's fault feature information is mined to determine the early fault occurrence node, namely the starting point of RUL prediction. Finally, based on the TE-PF prediction method proposed in this paper, the RUL prediction results of bearing under the probability interval are obtained. The experimental results also verified the effectiveness of the proposed method. However, experimental verification shows that the particle depletion phenomenon still exists in the TE-PF method, which will be further studied in the future.

ACKNOWLEDGEMENTS

This work is supported by the National Key Research and Development Program of China (No. 2018YFB1702401), National Natural Science Foundation of China (Grant No. 51975576, 51475463).

The authors are grateful for the helpful comments and constructive suggestions of the journal editors and anonymous reviewers.

CONFLICT OF INTEREST STATEMENT

The authors declare no conflicts of interest.

References

[1] P Luo, N. Q. Hu, and L. Zhang, "Improved phase space warping method for degradation tracking of rotating machinery under variable working conditions," *Mech. Syst. Signal Process.*, vol. 157, pp. 107696–107716, 2021.

[2] D. Zhao, T. Wang, and F. Chu, "Deep convolutional neural network based planet bearing fault classification," *Comput. Ind.*, vol. 107, pp. 59–66, 2019.

[3] S. Dong and T. Luo, "Bearing degradation process prediction based on the PCA and optimized LS-SVM model," *Measurement*, vol. 46, pp. 3143–3152, 2013.

[4] X. Li, W. Zhang, and Q. Ding, "Deep learning-based remaining useful life estimation of bearings using multi-scale feature extraction," *Reliab. Eng. Syst. Saf.*, vol. 182, pp. 208–218, 2019.

[5] Q. Niu, S. Yang, and C. Gan, "A modified phase space warping method for tracking damage evolution of rotating machineries," *J. Vib/ Shock*, vol. 38, pp. 14–21, 2019.

[6] T. Barszcz and N. Sawalhi, "Fault detection enhancement in rolling element bearings using the minimum entropy deconvolution," *Arch. Acoust.*, vol. 37, pp. 11–18, 2012.

Table 5. Comparison results of PF prediction performance under different observation sample duration

	Duration of observed sample 2700 s		Duration of observed sample 10 400 s	
Methods	**Prognosis accuracy (%)**	**Computing time (s)**	**Prognosis accuracy (%)**	**Computing time (s)**
Standard PF	53.28	14.29	89.14	11.85
DRT-PF	44.22	4.12	86.64	5.82
TE-PF	44.53	4.03	96.02	7.16

[7] Y. Lei, N. Li, and L. Guo, "Machinery health prognostics: a systematic review from data acquisition to RUL prediction," *Mech. Syst. Signal Process.*, vol. 104, pp. 799–834, 2018.
[8] Z. Huang, Z. Xu, X. Ke, et al. "Remaining useful life prediction for an adaptive skew-Wiener process model," *Mech. Syst. Signal Process.*, vol. 87,no. PT.A, pp. 294–306, 2017.
[9] A. Malhi, R. Yan, and R. Gao, "Prognosis of defect propagation based on recurrent neural networks," *IEEE Trans. Instrum. Meas.*, vol. 60, pp. 703–711, 2011.
[10] J. Ryue and P. R. White, "The detection of cracks in beams using chaotic excitations," *J. Sound Vib.*, vol. 307, pp. 627–638, 2007.
[11] B. Fan, *Research on Fault Prediction Method for Health Management of Aircraft Key Components*: National University of Defense Technology, 2015.
[12] P. Luo, N. Q. Hu, and L. Zhang, "Adaptive Fisher-based deep convolutional neural network and its application to recognition of rolling element bearing fault patterns and sizes," *Math. Probl. in. Eng.*, vol. 2020, pp. 1–11, 2020.
[13] N .Q. Hu, H. P. Chen, and Z. Cheng, "Fault diagnosis method of planetary gearbox based on empirical mode decomposition and deep convolutional neural network," *J. Mech. Eng.*, vol. 55, pp. 9–18, 2019.
[14] P. Luo, N. Q. Hu, and G. Q. Shen, "Intelligent FLHI extraction method for rolling bearings based on 1DDCNN and PCA information fusion," *J. Vib. Shock*, vol. 40, pp. 143–149, 2021.
[15] L. He, *Research on Gear Fault Enhancement Detection Based on Minimum Entropy Deconvolution*; National University of Defense Technology, 2017.
[16] H. Endo and R. B. Randall, "Enhancement of autoregressive model based gear tooth fault detection technique by the use of minimum entropy deconvolution filter," *Mech. Syst. Signal Process.*, vol. 21, pp. 906–919, 2007.
[17] L. Zhang, J. Y. Yi, and G. L. Xiong, "Early fault feature extraction of rolling bearing based on MED and TQWT," *Mech. Sci. Technol.*, vol. 40,p. 7, 2021.
[18] G. L. Mcdonald, Q. Zhao, and M. J. Zuo, "Maximum correlated kurtosis deconvolution and application on gear tooth chip fault detection," *Mech. Syst. Signal Process.*, vol. 33, pp. 237–255, 2012.
[19] X. Y. Zhu and Y. J. Wang, "Early fault diagnosis of rolling bearings based on autocorrelation analysis and MCKD," *J. Vib. Shock*, vol. 38, pp. 183–188, 2019.
[20] G. L. Mcdonald and Q. Zhao, "Multipoint optimal minimum entropy deconvolution and convolution fix: application to vibration fault detection," *Mech. Syst. Signal Process.*, vol. 82, pp. 461–477, 2017.
[21] J. Z. Xia, M. Q. Yu, and B. Y. Chuan, "Rolling bearing fault feature extraction based on improved information graph and MOMEDA," *J. Vib/ Shock*, vol. 38, pp. 26–32, 2019.
[22] D. Acuna, and M. Orchard, "Particle-filtering-based failure prognosis via sigma-points: Application to Lithium-Ion battery State-of-Charge monitoring." *Mech. syst. Signal. Process.*, vol. 85, pp. 827–848, 2017.
[23] Y. Luo, D. Liu, and Y. Peng, "Uncertainty Processing in Prognostics and Health Management: An Overview." 2012 Prognostics and System Health Management Conference, Beijing, China, pp. 5: 1–6, 2012.
[24] Q. Miao, H. J. Cui, and Xie, "Application of particle filter in residual life prediction of lithium ion battery," *J. Chongqing Univ.: Nat. Sci.*, vol. 36, pp. 47–52, 2013.
[25] M. N. Wang, W. Niu, and Y Y. Zhao, "Residual life prediction method of enhanced particle filter based on degradation trajectory," *Inf. Technol. Inform.*, vol. 6, pp. 59–61, 2021.
[26] Y. Qian and R. Yan, "Remaining useful life prediction of rolling bearings using an enhanced particle filter," *IEEE Trans. Instrum. Meas.*, vol. 64,p. 1, 2015.
[27] A. Hr, A. Fj, C. Apa, et al. "A method for the reduction of the computational cost associated with the implementation of particle-filter-based failure prognostic algorithms," *Mech. Syst. Signal Process.*, vol. 135, pp. 106421, 2020.
[28] J. Chen, S. Yuan, and X. Jin, "On-line prognosis of fatigue cracking via a regularized particle filter and guided wave monitoring," *Mech. Syst. Signal Process.*, vol. 131, pp. 1–17, 2019.
[29] J. Chen, S. Yuan, and H. Wang, "On-line updating Gaussian process measurement model for crack prognosis using the particle filter," *Mech. Syst. Signal Process.*, vol. 140, p. 106646, 2020.
[30] M. Corbetta, C. Sbarufatti, M. Giglio, et al. "Optimization of nonlinear, non-Gaussian Bayesian filtering for diagnosis and prognosis of monotonic degradation processes," *Mech. Syst. Signal Process.*, vol. 104, pp. 305–322, 2018.
[31] D. E. Acuna and M. E. Orchard, "Particle-filtering-based failure prognosis via sigma-points: application to Lithium-Ion battery State-of-Charge monitoring," *Mech. Syst. Signal Process.*, vol. 85, pp. 827–848, 2017.
[32] H. Yu and H. Li, "Pump remaining useful life prediction based on multi-source fusion and monotonicity-constrained particle filtering," *Mech. Syst. Signal Process.*, vol. 170, p. 108851, 2022.
[33] H. Wei, N. Williard, M. Osterman, et al. "Prognostics of lithium-ion batteries based on Dempster–Shafer theory and the Bayesian Monte Carlo method," *J. Power Sources*, vol. 196, pp. 10314–10321, 2011.